Shiraz University

IJVR

ISSN: 1728-1997 (Print)
ISSN: 2252-0589 (Online)

Vol. 22 No. 2 Ser. No. 75 2021

IRANIAN JOURNAL OF VETERINARY RESEARCH

Short Paper

Three dimensional modeling and quantitative analysis of long bone parameters of rabbit using micro-computed tomography

Bakici, C.[1*]; Akgun, R. O.[2]; Ekim, O.[1]; Batur, B.[3]; Bakici, M.[4]; Ozen, D.[5] and Soydal, C.[6]

[1]Department of Anatomy, Faculty of Veterinary Medicine, Ankara University, Ankara, Turkey; [2]Department of Basic Sciences, Faculty of Dentistry, Cankiri Karatekin University, Cankiri, Turkey; [3]MSc Student in Anatomy, Department of Anatomy, Faculty of Veterinary Medicine, Ankara University, Ankara, Turkey; [4]Department of Surgery, Faculty of Veterinary Medicine, Kırıkkale University, Kırıkkale, Turkey; [5]Department of Biostatistics, Faculty of Veterinary Medicine, Ankara University, Ankara, Turkey; [6]Department of Nuclear Medicine, Faculty of Medicine, Ankara University, Ankara, Turkey

[*]***Correspondence:*** *C. Bakici, Department of Anatomy, Faculty of Veterinary Medicine, Ankara University, Ankara, Turkey. E-mail: vetcanerbakici@gmail.com*

10.22099/ijvr.2021.39092.5688

(Received 22 Nov 2020; revised version 13 Feb 2021; accepted 21 Feb 2021)

Abstract

Background: Micro-computed tomography (μCT), a modern imaging technique, provides detailed information on the bone morphology of small animal models. **Aims:** The objectives are 1) to produce three dimensional (3D) models from μCT images of femoral and tibial bones of New Zealand rabbits, and 2) to estimate and compare morphometric and volumetric results among genders as well as left and right sides. **Methods:** A total of twenty adult New Zealand rabbits (10 females, 10 males, aged 12-18 weeks, weight= 2.5-3 kg) were used for this study. Three dimensional reconstructed models of the femoral and tibial bones of rabbits were created from cross-sectional images of μCT using the 3D Slicer program. Anatomical structures were determined on these 3D bone models. Afterward, morphometric parameters such as length, thickness, and width of various parts of the bones were calculated with volume and volume ratio values of cortical bone, trabecular bone, and medullary cavity. **Results:** The gender*laterality interaction term was found statistically significant in measurements of femoral diaphysis diameter (FDD), internal femoral diaphysis diameter (IFDD), femoral head diameter (FHD), tibial diaphysis diameter (TDD), tibial distal width (TDH), and tibial proximal width (TPW) ($P<0.001$). The gender*laterality interaction term was not significant in volume and volume fraction values of cortical bone, trabecular bone, and medullary cavity ($P>0.05$). **Conclusion:** It is thought that the study will contribute to the orthopedic experimental studies of rabbits for femoral and tibial bones and will bring a modern perspective to the field of veterinary anatomy.

Key words: Femur, Micro-computed tomography, Morphometry, Three-dimensional reconstruction, Tibia

Introduction

As a laboratory animal, rabbit (*Oryctolagus cuniculus L.*) is especially assigned in orthopedic researches as well as biomedical, immunology, and genetics studies. New Zealand rabbit, Dutch Belted rabbit, and Flemish Giant rabbit breeds are the most common animals used in laboratory studies (Brewer, 2006). In osteomorphometric studies on rabbits, the normal anatomical features of the bones involve essential information (Ajayi *et al*., 2012). In morphometric studies, rabbits are preferred instead of small rodents that can easily be applied for size parameters or density measurements provided by the imaging techniques on long bones (Pazzaglia *et al*., 2010).

In recent years, computed tomography (CT) imaging has been widely allocated to evaluate bone morphometry in veterinary medicine. Thus, a detailed evaluation of bone structures and calculation of quantitative data of desired structures has already been made (Zotti *et al*., 2009; Bagi *et al*., 2011; Özkadif *et al*., 2016). The long bones structures of rabbits can be examined very easily in such imaging techniques (Pazzaglia *et al*., 2010). By developing technology, progress in imaging techniques provide benefits in many fields, especially in medicine. Micro-computed tomography (μCT), a modern imaging technique, provides detailed information on the bone morphology of small animal models (Jiang *et al*., 2000; Bagi *et al*., 2011). Through these models, complex anatomical structures can be well defined and the localization of formations can be easily identified (Estai and Bunt, 2016; Kubikova *et al*., 2018). In addition, biometric measurements can be obtained easily from the three dimensional (3D) model of these anatomical structures. The accuracy and reliability of linear and angular measurements on 3D models have been clearly defined (Kim *et al*., 2012; Stull *et al*., 2014; Savio *et al*., 2016).

Several studies focused on long bone morphometry of rabbits have applied the morphometric measurement technique using digital caliper widely. (Pazvant and Kahvecioglu, 2009; Ajayi *et al*., 2012). Our study was aimed to obtain the 3D models of rabbit femoral and tibial bones using µCT images. Micro-computed tomography imaging can be quite effective to obtain high-resolution bone tissue images, especially to estimate the length and volume measurements of images and 3D models, and to evaluate statistical differences between genders as well as left and right sides.

Materials and Methods

A total of 20 (10 females, 10 males) New Zealand rabbits (aged range of 12-18 weeks) weighing from 2.5 to 3 kg were used in the study. This study was approved by XXX University Local Ethics Committee for Animal Experiments (decision No. 2020-5-44). Bones were collected from cadaveric rabbits euthanized in other experiments, not related to bone or bone metabolism.

The cross-sectional images were acquired from a µCT device (Super Argus PET/CT, Sedecal, Spain) at a value of 40 kV, 140 µA, and a thickness of 0.12 mm (Bouxsein *et al.*, 2010). In order to perform a 3D reconstruction on the cross-sectional images, they were transferred to a 3D Slicer (3D Slicer, GitHub, San Francisco) software program. Cortical tissue, cancellous tissue, and medullary cavity of the bones were segmented on cross-sectional images, and 3D models of the bone tissues were formed. The segmentation process was carried out by the "Segment editor" function. The volume intensity value were ranged from 4800-7400 (for cortical tissue) to 1300-2800 (for cancellous tissue) for 3D reconstructed models. The three dimensional models were created by "Grow from seeds" function from the segmented cross-sectional images. Undesired or false segmentation processes were remodeled at this stage. Thereafter, final 3D models were generated by "Show 3D" function. The cortical tissue volume (CTV), cancellous tissue volume (CaTV), and medullar cavity volume (MCV) were estimated by "Label statistics" function (Fedorov *et al.*, 2012). The cortical tissue volume fraction (CTVF), cancellous tissue volume fraction (CaTVF), medullar cavity volume fraction (MCVF) values of the femoral, and tibial bones were estimated by dividing the desired region to a total region.

Anatomical structures were defined and termed for 3D images; the measurements and the index values, as in previous researches, were also calculated. The definitions are given in Table 1 (von den Driesch, 1976; Pazvant and Kahvecioglu, 2009; Özkadif *et al.*, 2016).

Descriptive statistics for each variable were calculated and presented as mean±SEM. For hypothesis testing, the data were subjected to two-way mixed ANOVA (analysis of variance). The model included "gender" (male-female) and "laterality" (right-left) as the main effects and "gender*laterality" interaction effects. Bonferroni corrected pairwise comparisons were performed for significant main effect terms in the model to evaluate differences among the levels within each factor when the interaction term was not significant. Simple effect analyses with Bonferroni adjustment were performed for significant interaction terms. A value less than 0.05 was considered significant. SPSS version 14.01 (License No. 9869264) was used for statistical analysis.

Results

Three dimensional models of rabbit femoral and tibial bones were created from µCT images. Anatomical structures could easily be determined by these models (Figs. 1 and 2).

Morphometric measurements were calculated from 3D models after the anatomical structures of the femoral and tibial bones were determined. The statistical data were obtained from the measurements given in Tables 2 and 3. The gender*laterality interaction term was found statistically significant for FDD, IFFD, FHD, TTW, TDD, TDW, TPW, and TL that means any change in the simple main effects of gender over left or right sides. However, FDW, FPW, and FL values were statistically significant for the gender effect indicating that the calculated values of females were significantly higher than the males for both sides. The gender*laterality interaction term was found statistically significant in the values of index 1 for femur bone and index 2 for both bones (Table 2).

Statistical analysis of the volume and volume fraction values of the image-based measurements is given in Table 3. There was a significant gender effect for tibial and femoral bone values of CTV and MCV. Although

Table 1: The name, abbreviation, and definition of the morphometric values for µCT images

Name	Abbreviation	Definition
Femoral diaphysis diameter	FDD	Transverse diaphysis diameter at the middle of the femur
Internal femoral diaphysis diameter	IFDD	Transverse diameter of the medullary cavity at the middle of the femur
Femoral proximal width	FPW	The maximum distance between the femoral head to the greater trochanter
Femoral head diameter	FHD	The maximum diameter at the middle of the femoral head
Femoral distal width	FDW	The maximum distance across the femoral condyles
Femoral length	FL	The maximum length of the femur
Tibial diaphysis diameter	TDD	Transverse diaphysis diameter at the middle of the tibia
Internal tibial diaphysis diameter	ITDD	Transverse diameter of the medullary cavity at the middle of the tibia
Tibial proximal width	TPW	The maximum distance at the proximal articular surface
Third trochanter width	TTW	The maximum distance across the third trochanter in the transversal plane
Tibial distal width	TDW	The maximum distance across the tibial malleolus in the transversal plane
Tibial length	TL	The maximum length of the tibia

µCT: Micro-computed tomography

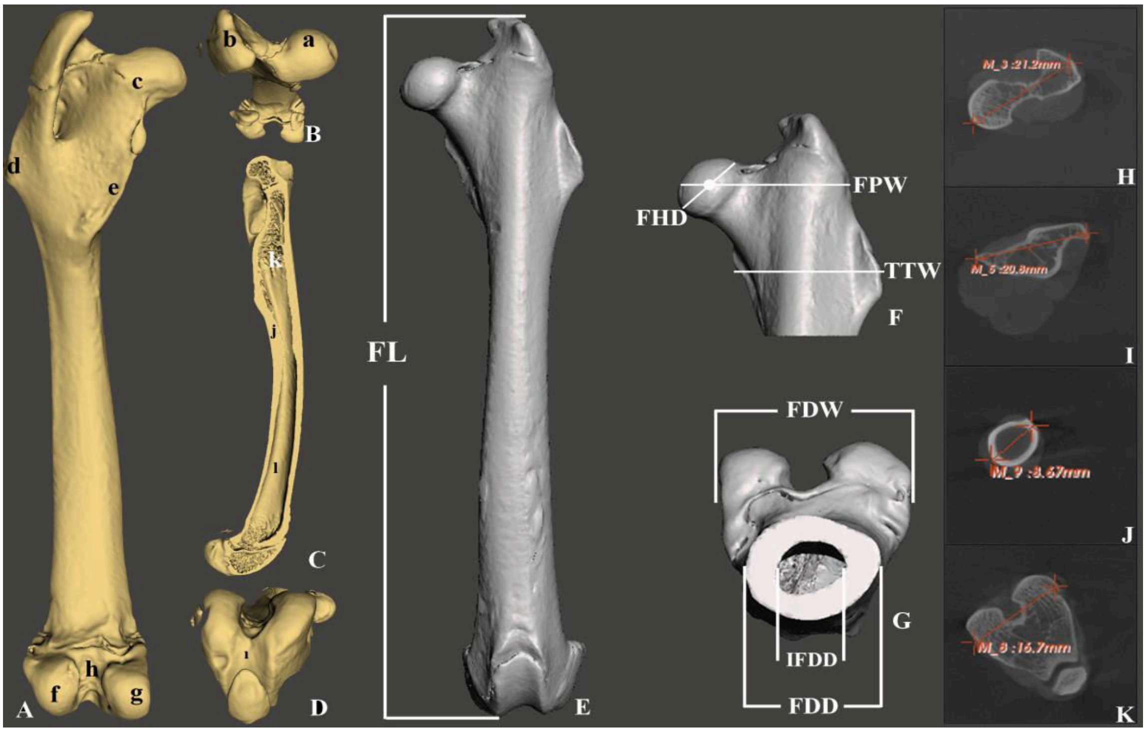

Fig. 1: Anatomical structures obtained from µCT 3D images of the femoral bone of the rabbit (**A**, **B**, **C**, and **D**), measurement points on the 3D models (**E**, **F**, and **G**), and cross-section views of the µCT images (**H**, **I**, **J**, and **K**). a: Head of the femoral bone, b: Greater trochanter, c: Neck of the femoral bone, d: Lesser trochanter, e: Third trochanter, f: Lateral condyle, g: Medial condyle, h: Intercondylar fossa, i: Trochlea of the femoral bone, j: Cortical bone, k: Cancellous bone, l: Medullary cavity, FL: Femoral length, FHD: Femoral head diameter, FPW: Femoral proximal width, TTW: Third trochanter width, FDW: Femoral distal width, IFDD: Internal femoral diaphysis diameter, and FDD: Femoral diaphysis diameter

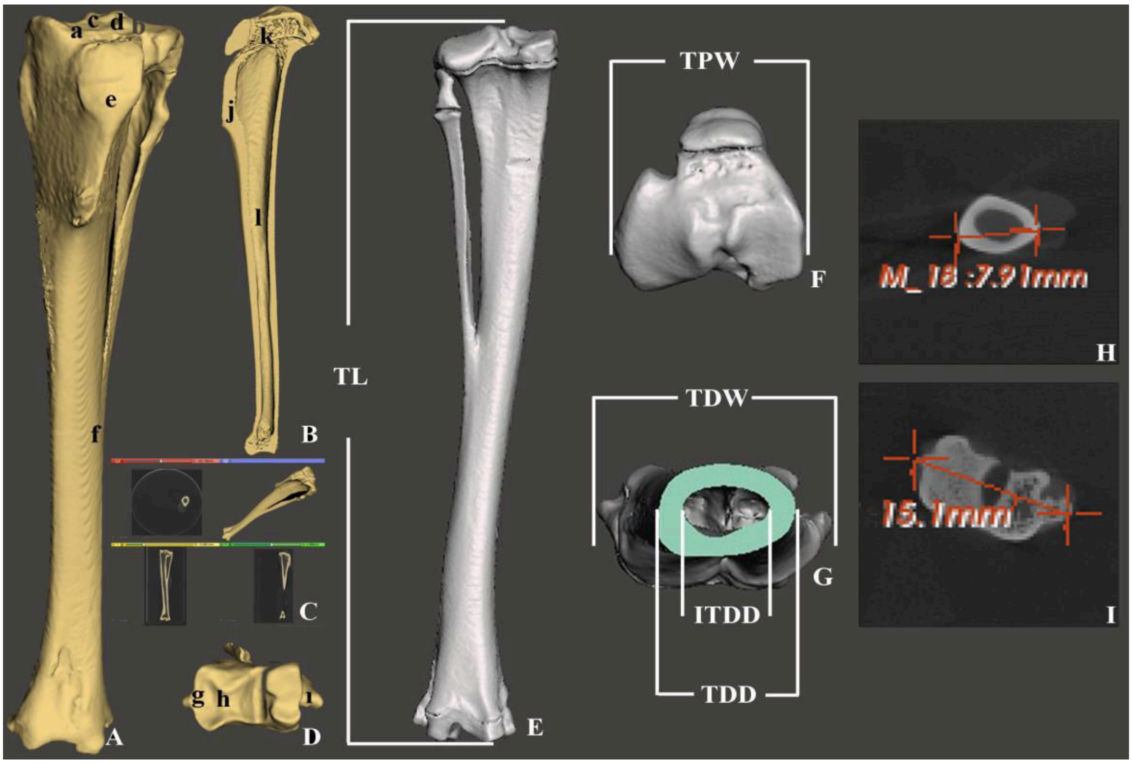

Fig. 2: Anatomical structures obtained from µCT 3D images of the tibial bone of the rabbit (**A**, **B**, **C**, and **D**), measurement points on the 3D models (**E**, **F**, and **G**), and cross-section views of the µCT images (**H** and **I**). a: Medial condyle, b: Lateral condyle, c: Medial intercondylar tubercle, d: Lateral intercondylar tubercle, e: Tibial tuberosity, f: Tibial shaft, g: Medial malleolus, h: Tibial cochlea, i: Lateral malleolus, j: Cortical bone, k: Cancellous bone, l: Medullary cavity, TL: Tibial length, TPW: Tibial proximal width, TDW: Tibial distal width, ITDD: Internal tibial diaphysis diameter, and TDD: Tibial diaphysis diameter

Table 2: The statistical results of morphometric values of the image-based measurements from µCT 3D reconstruction models of the bones (mm)

Measurement		Gender	Laterality		P-value		
			Right	Left	Gender	Laterality	Gender × Laterality
FDD		F	8.57 ± 0.02$^{A, a}$	8.45 ± 0.03$^{B, a}$	<0.001	<0.001	<0.001
		M	8.22 ± 0.03$^{A, b}$	7.13 ± 0.03$^{B, b}$			
IFDD		F	6.04 ± 0.01$^{A, a}$	6 ± 0.01$^{A, a}$	<0.001	<0.001	<0.001
		M	5.77 ± 0.03$^{A, b}$	4.68 ± 0.007$^{B, b}$			
FDW		F	15.9 ± 0.21^{a}	15.96 ± 0.3^{a}	<0.001	0.592	0.423
		M	14.31 ± 0.12^{b}	14.35 ± 0.08^{b}			
FHD		F	8.95 ± 0.08$^{A, a}$	8.83 ± 0.02$^{A, a}$	<0.001	<0.001	<0.001
		M	8.78 ± 0.03$^{A, a}$	7.86 ± 0.07$^{B, b}$			
FPW		F	20.46 ± 0.2^{a}	19.93 ± 0.31^{a}	<0.001	0.167	0.138
		M	17.84 ± 0.12^{b}	17.86 ± 0.12^{b}			
FL		F	95.78 ± 0.44^{a}	95.66 ± 0.57^{a}	<0.001	0.869	0.623
		M	91.41 ± 0.26^{b}	91.65 ± 0.12^{b}			
TTW		F	20.31 ± 0.1$^{A, a}$	20.17 ± 0.32$^{A, a}$	<0.001	0.018	0.049
		M	18.39 ± 0.13$^{A, b}$	17.59 ± 0.12$^{B, b}$			
TDD		F	7.38 ± 0.11$^{A, a}$	7.39 ± 0.1$^{A, a}$	<0.001	0.001	0.001
		M	6.79 ± 0.03$^{A, b}$	6.34 ± 0.05$^{B, b}$			
ITDD		F	4.39 ± 0.07^{A}	4.23 ± 0.06^{B}	0.721	0.032	0.768
		M	4.38 ± 0.1^{A}	4.17 ± 0.11^{B}			
TDW		F	12.41 ± 0.08$^{A, a}$	12.31 ± 0.06$^{A, a}$	<0.001	<0.001	0.002
		M	12.09 ± 0.04$^{A, b}$	11.57 ± 0.06$^{B, b}$			
TPW		F	17.72 ± 0.06$^{A, a}$	18.16 ± 0.07$^{B, a}$	<0.001	0.049	<0.001
		M	17.31 ± 0.08$^{A, b}$	16.61 ± 0.05$^{B, b}$			
TL		F	107.78 ± 0.29$^{A, a}$	106.75 ± 0.46$^{B, a}$	<0.001	0.703	0.002
		M	100.02 ± 0.2$^{A, b}$	102.8 ± 0.34$^{A, b}$			
Femur	Index 1 (%)	F	29.55 ± 0.13$^{A, a}$	28.98 ± 0.33$^{A, a}$	<0.001	<0.001	<0.001
		M	29.73 ± 0.3$^{A, a}$	34.28 ± 0.83$^{B, b}$			
	Index 2 (%)	F	8.95 ± 0.03$^{A, a}$	8.84 ± 0.06$^{A, a}$	<0.001	<0.001	<0.001
		M	8.99 ± 0.03$^{A, a}$	7.77 ± 0.03$^{B, b}$			
Tibia	Index 1 (%)	F	40.5 ± 0.4^{a}	42.75 ± 0.92^{a}	<0.001	0.62	0.131
		M	35.47 ± 1.4^{b}	34.32 ± 1.36^{b}			
	Index 2 (%)	F	6.85 ± 0.08$^{A, a}$	6.92 ± 0.08$^{A, a}$	<0.001	<0.001	<0.001
		M	6.75 ± 0.03$^{A, a}$	6.23 ± 0.06$^{B, b}$			

^{ab} Different superscripts in the same column represents a statistically significant difference (P<0.05), and ^{AB} Different superscripts in the same row represents a statistically significant difference (P<0.05). µCT: Micro-computed tomography, 3D: Three dimensional, FDD: Femoral diaphysis diameter, IFDD: Internal femoral diaphysis diameter, FDW: Femoral distal width, FHD: Femoral head diameter, FPW: Femoral proximal width, FL: Femoral length, TTW: Third trochanter width, TDD: Tibial diaphysis diameter, ITDD: Internal tibial diaphysis diameter, TDW: Tibial distal width, TPW: Tibial proximal width, TL: Tibial length, F: Female, and M: Male

calculated volumes of femoral and tibial bone CaTV were found higher in females than males, the differences were not statistically significant for the tibial bone (P>0.05). Also, statistically differences were shown in femoral bone values of CTVF and MCVF, and tibial bone value of CaTVF in the gender effect (P<0.05).

Discussion

The skeletal system is mechanically optimized in biology. Commonly, the mechanical properties of bone can be defined by various parameters such as geometric structures, mineral density, and the amount of cortical and cancellous bone tissue (Bagi *et al.*, 2011). For instance, the rabbit skull has a large amount of cancellous bone structure (Brewer, 2006). Bagi *et al.* (2011) evaluated the bone volume of rabbit femur from the sectional image of µCT. In our study, the whole volume and volume fraction values of cortical bone, cancellous bone, and medullary cavity of femoral and tibial bones were estimated in both specimens. It was found that gender*laterality interaction term was not significant in volume fraction values of cortical bone, trabecular bone, and medullary cavity (P>0.05). However, CTV, CaTV, MCV, CTVF, and MCVF values of the femoral bone, and CTV, MCV, and CaTVF values of the tibial bone were found significant between genders (P<0.05).

Table 3: The statistical results of the volume and volume fraction values of the image-based measurements on µCT 3D reconstruction models of the bones (mm^3)

	Measurement	Gender	Laterality		P-value		
			Right	Left	Gender	Laterality	Gender × Laterality
Femur	CTV	F	3054.4 ± 48.6[a]	2997.55 ± 53.17[a]	<0.001	0.194	0.448
		M	2715.46 ± 22.21[b]	2700.14 ± 21.08[b]			
	CaTV	F	1612.05 ± 72.17[a]	1616.95 ± 66.58[a]	0.004	0.799	0.654
		M	1373.25 ± 43.39[b]	1355.48 ± 39.97[b]			
	MCV	F	1945.83 ± 69.19[a]	1957.17 ± 78.82[a]	0.001	0.859	0.699
		M	1302.91 ± 28.35[b]	1363.06 ± 48.87[b]			
Tibia	CTV	F	2770.14 ± 30.23[a]	2802.11 ± 39.16[a]	<0.001	0.82	0.052
		M	2397 ± 35.8[b]	2357.05 ± 25.9[b]			
	CaTV	F	869.69 ± 42.25	928.46 ± 34.17	0.101	0.086	0.11
		M	830.57 ± 19.27	832.84 ± 16.9			
	MCV	F	1541.17 ± 76.1[a]	1618.98 ± 57.71[a]	<0.001	0.263	0.294
		M	1288.15 ± 38.49[b]	1290.71 ± 24.68[b]			
Femur	CTVF	F	0.47 ± 0.01[a]	0.46 ± 0.01[a]	<0.001	0.067	0.523
		M	0.5 ± 0.01[b]	0.5 ± 0.01[b]			
	CaTVF	F	0.24 ± 0.001	0.25 ± 0.01	0.221	0.999	0.357
		M	0.25 ± 0.01	0.25 ± 0.001			
	MCVF	F	0.3 ± 0.001[a]	0.3 ± 0.01[a]	<0.001	0.137	0.314
		M	0.24 ± 0.01[b]	0.25 ± 0.01[b]			
Tibia	CTVF	F	0.54 ± 0.01	0.53 ± 0.01	0.789	0.2	0.663
		M	0.53 ± 0.01	0.53 ± 0.01			
	CaTVF	F	0.17 ± 0.001[a]	0.17 ± 0.001[a]	0.002	0.106	0.45
		M	0.18 ± 0.001[b]	0.19 ± 0.001[b]			
	MCVF	F	0.3 ± 0.01	0.3 ± 0.01	0.124	0.376	0.766
		M	0.29 ± 0.01	0.29 ± 0.01			

[ab] Different superscripts in the same column represents a statistically significant difference ($P<0.05$), and [AB] Different superscripts in the same row represents a statistically significant difference ($P<0.05$). µCT: Micro-computed tomography, 3D: Three dimensional, CTV: Cortical tissue volume, CaTV: Cancellous tissue volume, MCV: Medullar cavity volume, CTVF: Cortical tissue volume fraction, CaTVF: Cancellous tissue volume fraction, MCVF: Medullar cavity volume fraction, F: Female, and M: Male

In this study, the greater trochanter was higher than the femoral head in both genders. The lesser trochanter projected dorsomedial and the well-developed third trochanter located on the proximal one-third of the length of the femur (Fig. 1). The properties of these three trochanters were similar to Ajayi *et al*. (2011) study reporting that the trochanter morphologies were characterized in specialized runner and jumper species. Wang *et al*. (2009) reported that the trochanteric fossa was very deep in male rabbits; Araujo *et al*. (2013) observed that the deep trochanteric fossa was found in laboratory rat, domestic guinea pigs, capybara, and lowland paca. In this study, the trochanteric fossa was deep in both genders and discovered in 2-dimensional (2D) section images and 3D reconstruction models. Ajayi *et al*. (2011) evaluated the morphometry of the femur with Vernier caliper in which results were divided based on right and left side. In our study, femoral bone of male and female rabbits were relatively longer than a previous study, however, the values of males were closer than the female results (Ajayi *et al*., 2011). Besides, the mean length of femoral bone and width of distal femoral bone of this study were similar to Pazvant and Kahvecioglu (2009) in both genders. But the mean width at the middle of the femoral head in both genders and the width of the proximal femoral bone in females were higher than their study. Overall, the index values of female rabbits were higher than the male rabbits and therefore the females had higher bone density, according to previous studies. In this study, females had higher tibial index 1 and index 2 values than males, and the results are similar to those of Pazvant and Kahvecioglu (2009).

It has been reported that the tibial and fibular bones of the New Zealand White rabbit are approximately fused in half of the tibia; the fusion are also shown in digger and leaper species (Brewer, 2006; Ajayi *et al*., 2011). In our study, this fusion was also found between tibial and fibular bones of both genders. The widths of distal tibia of male and female rabbits were similar to Ajayi *et al*. (2011). It was stated that the relatively short femoral bone compared to the tibial bone in absolute terms was consistent with that of runners (Ajayi *et al*., 2011). Their results comply with our study. The length of the tibial bone was longer than the length of the femoral bone in both genders. In this study, the mean length of the tibial bone and the mean diameter of the left tibial shaft in males were similar to Pazvant and Kahvecioglu (2009) report. But the mean length of the tibial bone, the mean diameter of the left tibial shaft in females, and the mean width of the proximal tibial bone in both genders were higher than Pazvant and Kahvecioglu (2009). The mean width of distal tibial bone in both genders was smaller than their investigation. Furthermore, the females had higher index 2 values than males, and the results are similar to those of Pazvant and Kahvecioglu (2009).

In normal and pathological conditions, µCT is used to evaluate the gross and micro-anatomy of the skeleton. µCT used in preclinical to clinical sciences provides a fast and reliable evaluation for bone morphology, the complex structure of the cortical and cancellous bone, and bone mineral density (Jiang *et al*., 2000; Pazvant and Kahvecioglu, 2009; Bagi *et al*., 2011). Comparing to histological method, µCT provides a 3D approach by preserving tissue samples. So, it has been used in metabolic bone diseases and bone tissue quantification studies. Micro-computed tomography is a technique that enables 3D visualization of cortical and cancellous bone structures in detail. Thus, the desired calculations can be applied easily. The disadvantage of µCT compared to histological studies is that it has a lower resolution than optical microscopy (Jiang *et al*., 2000; Hoechel *et al*., 2015; Kubikova *et al*., 2018). In parallel with the previous studies, our µCT findings provided information on bone tissue in detail, and the cortical and cancellous tissue of the bones were visualized in high detail. Further, the the desired regions were calculated easily on these 2D and 3D images. It is reported that 3D models created through µCT images can overcome deficiencies of 2D approaches.

In conclusion, the anatomy and morphometric data of the similarities or differences among the genders are very important. The study involves a 3D approach and accurate morphometric data to the structures of femoral and tibial bone. We hope that our findings will present the advantages of 3D modeling, preoperative and postoperative planning, morphometric researches, orthopedic implant designs, and surgical approaches.

Conflict of interest

The authors declare that they do not have any conflict of interest.

References

Ajayi, IE; Shawulu, JC; Zachariya, TS; Ahmed, S and Adah, BM (2012). Osteomorphometry of the bones of the thigh, crus and foot in the New Zealand white rabbit (*Oryctolagus cuniculus*). Ital. J. Anat. Embryol., 117: 125-134.

Araujo, FAP; Sesoko, NF; Rahal, SC; Teixeira, CR; Müller, TR and Machado, MRF (2013). Bone morphology of the hind limbs in two caviomorph rodents. Anat. Histol. Embryol., 42: 114-123.

Bagi, CM; Berryman, E and Moalli, MR (2011). Comparative bone anatomy of commonly used laboratory animals: Implications for drug discovery. Comp. Med., 61: 76-85.

Bouxsein, ML; Boyd, SK; Christiansen, BA; Guldberg, RE; Jepsen, KJ and Müller, R (2010). Guidelines for assessment of bone microstructure in rodents using micro-computed tomography. J. Bone Miner Res., 25: 1468-1486.

Brewer, NR (2006). Biology of the rabbit. J. Am. Assoc. Lab. Anim. Sci., 45: 8-24.

Estai, M and Bunt, S (2016). Best teaching practices in anatomy education: A critical review. Ann. Anat., 208: 151-157.

Fedorov, A; Beichel, R; Kalpathy-Cramer, J; Finet, J; Fillion-Robin, JC; Pujol, S; Bauer, C; Jennings, D; Fennessy, F; Sonka, M; Buatti, J; Aylward, S; Miller, JV; Pieper, S and Kikinis, R (2012). 3D slicer as an image computing platform for the quantitative imaging network. Magn. Reson. Imagin., 30: 1323-1341.

Hoechel, S; Schulz, G and Gerbl, MM (2015). Insight into the 3D-trabecular architecture of the human patella. Ann. Anat., 200: 98-104.

Jiang, Y; Zhao, J; White, DL and Genant, HK (2000). Micro CT and Micro MR imaging of 3D architecture of animal skeleton. J. Musculoskel. Neuron. Interact., 1: 45-51.

Kim, M; Huh, KH; Yi, WJ; Heo, MS; Lee, SS and Choi, SC (2012). Evaluation of accuracy of 3D reconstruction images using multi-detector CT and cone-beam CT. Imaging Sci. Dent., 42: 25-33.

Kubikova, T; Bartos, M; Juhas, S; Suchy, T; Sauerova, P; Kalbacova, MH and Tonar, Z (2018). Comparison of ground sections, paraffin sections and micro-CT imaging of bone from the epiphysis of the porcine femur for morphometric evaluation. Ann. Anat., 220: 85-96.

Pazvant, G and Kahvecioglu, KO (2009). Studies on homotypic variation of forelimb and hindlimb long bones of rabbits. J. Fac. Vet. Med. Istanbul. Univ., 35: 23-29.

Pazzaglia, UE; Zarattini, G; Giacomini, D; Rodella, L; Menti, AM and Feltrin, G (2010). Morphometric analysis of the canal system of cortical bone: an experimental study in the rabbit femur carried out with standard histology and micro-CT. Anat. Histol. Embryol., 39: 17-26.

Savio, G; Baroni, T; Concheri, G; Baroni, E; Meneghello, R; Longo, F and Isola, M (2016). Computation of femoral canine morphometric parameters in three-dimensional geometrical models. Vet. Surg., 45: 987-995.

Stull, KE; Tise, ML; Ali, Z and Fowler, DR (2014). Accuracy and reliability of measurements obtained from computed tomography 3D volume rendered images. Forensic Sci. Int., 238: 133-140.

von den Driesch, A (1976). *A guide to the measurement of animal bones from Archaeological sites*. 1st Edn., Cambridge, Massachusetts, Harvard University. PP: 84-87.

Wang, HH; Wang, YXJ; Sheng, H; Zhang, G; Qin, L; Ahuja, AT and Teng, LS (2009). Fossa trochanterica of the proximal femur in rabbits: an anatomic structure for potential misinterpretation on magnetic resonance images. Acta Radiol., 50: 212-216.

Zotti, A; Banzato, T and Cozzi, B (2009). Cross-sectional anatomy of the rabbit neck and trunk: Comparison of computed tomography and cadaver anatomy. Res. Vet. Sci., 87: 171-176.